

## First results from the MEG experiment

G. PIREDDA on behalf of the MEG COLLABORATION

*INFN, Sezione di Roma Sapienza - Rome, Italy*

(ricevuto il 14 Settembre 2010; pubblicato online il 13 Gennaio 2011)

**Summary.** — The MEG experiment, searching for the rare decay  $\mu^+ \rightarrow e^+\gamma$ , started the data taking at PSI in 2008. Based on data from the initial three months of operation an upper limit on the branching ratio  $\text{BR}(\mu \rightarrow e\gamma) < 2.8 \cdot 10^{-11}$  at 90% confidence level is reported. This corresponds to the measurement of positrons and photons from  $\sim 10^{14}$  stopped  $\mu^+$ -decays by a superconducting positron spectrometer and a 900 litre liquid-xenon photon detector.

PACS 13.35.-r – Decays of leptons.

PACS 13.35.Bv – Decays of muons.

### 1. – Introduction

The MEG experiment [1] aims at the search for the lepton flavor violating decay  $\mu \rightarrow e\gamma$  with a sensitivity of  $10^{-13}$  in the branching ratio, improving the current limit [2] by two orders of magnitude.

The long quest (see fig. 1) for the  $\mu \rightarrow e\gamma$  started many decades ago, in the forties of the 20th century. It is interesting to note that the search for the nowadays exotic decay marks different periods of the long process of building the Standard Model (SM) of the elementary particles. In fact in the pioneer search of the  $\mu \rightarrow e\gamma$  in the cosmic radiation, the goal was just to determine the nature of the recently ascertained  $\mu$  meson particle. Later on in the 60-ies pions at rest produced by the new accelerators were used and the lack of a signal at  $10^{-3}$  level was a clear indication of the existence of (at least) two neutrino species. Finally dedicated muon beams become available allowing better sensitivities able to set stringent constraints on new physics models. Let us notice that despite the  $\nu_\mu \rightarrow \nu_e$  oscillation has been established, yet the  $10^{-54}$  SM branching ratio prediction is experimentally out of reach. In extensions of SM, lepton flavor violation rates may become much larger [3, 4] and experimentally accessible. Hence improving existing experimental bounds, is of great relevance to search for new physics, especially on the very sensitive  $\mu \rightarrow e\gamma$  channel.

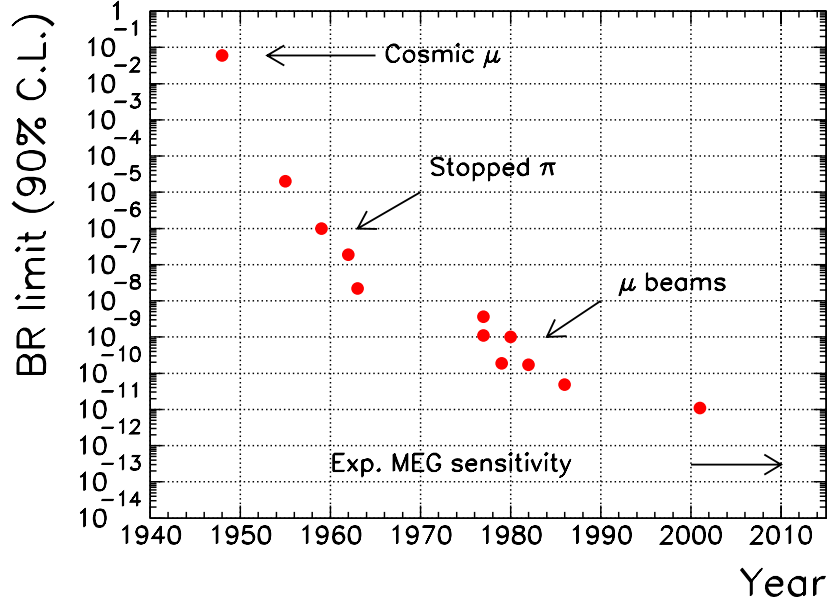


Fig. 1. – The  $\mu \rightarrow e\gamma$  upper limit as a function of the year. The MEG expected sensitivity is also shown.

## 2. – Signal signature and the backgrounds

The  $\mu \rightarrow e\gamma$  signal has a simple topology if the muon decays at rest, and appears as two-body final state of a positron and a  $\gamma$ -ray, emitted back-to-back with an energy of 52.8 MeV each, corresponding to half of the muon mass. The signal detection is, in principle, rather easy. One needs in fact to have a very intense continuous muon beam and to measure the positron and photon energies ( $E_e, E_\gamma$ ), the relative angle  $\theta_{e\gamma}$  and the time difference  $t_{e\gamma}$ . However to achieve the mentioned sensitivity, the following very high resolutions are needed:  $\delta E_e/E_e = 0.35\%$ ,  $\delta E_\gamma/E_\gamma = 1.8\%$ ,  $\delta t_{e\gamma} = 65$  ps,  $\delta\theta_{e\gamma} = 10$  mrad. These are very ambitious goals that can be achieved only with optimized detectors and very careful calibrations.

The backgrounds come from the radiative muon decay (RMD)  $\mu \rightarrow e\nu\nu\gamma$  and the accidental coincidences between a positron from the normal Michel decay ( $\mu \rightarrow e\nu\bar{\nu}$ ) and a high energy photon from RMD decay, positron annihilation in flight or bremsstrahlung. The accidental events dominate and it can be shown that the expected contribution is  $N_{acc} = R_\mu^2 (\Delta\theta_{e\gamma})^2 (\Delta E_\gamma)^2 \Delta t_{e\gamma} \Delta E_e$ , where  $R_\mu$  is the muon beam rate and the other terms are the resolutions on the measured observable already mentioned.

## 3. – The detector

The MEG experiment (fig. 2) is located at the Paul Scherrer Institut (PSI) in Switzerland and operates at the 590 MeV proton cyclotron. Three key elements enable the excellent sensitivity of the experiment: i) a high rate continuous muon (positive to avoid formation of muonic atoms and muon capture) beam, ii) an innovative liquid-xenon (LXe) scintillation  $\gamma$ -ray detector [5], and iii) a specially designed positron spectrometer [6] with a gradient magnetic field (0.4–1.2 T) and a scintillation timing-counter array

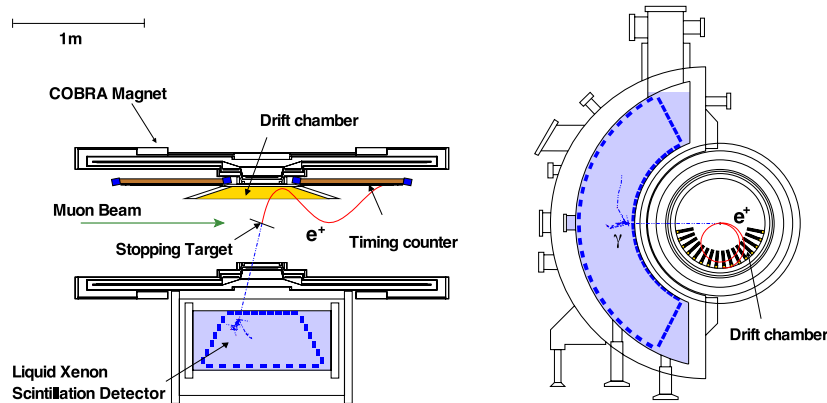


Fig. 2. – Top (left) and front (right) view of the MEG detector.

for fast timing and triggering [7].

Surface muons of  $28 \text{ MeV}/c$  from the  $\pi E5$  channel at PSI are stopped in a  $18 \text{ mg}/\text{cm}^2$  thin polyethylene target. The transport system, which includes a Wien filter and a superconducting transport solenoid, is able to separate to  $7.5 \sigma$  the eight time more abundant positron contamination to provide a pure muon beam. Positrons from the muons decaying in the target are detected by a system of drift chambers (DCH) immersed in a superconducting gradient field magnet. The magnet, ranging from  $1.27 \text{ T}$  at the center to  $0.49 \text{ T}$  at either end, has been designed in such a way that the trajectory of positron from the target with the same momentum is independent of the emission angle, optimizing the DCH acceptance and sweeping away low momentum particles more efficiently, compared to a uniform field.

The drift chambers are sixteen radial modules placed on a half circumference around the target. A module has two staggered layers of anode wire planes each of nine cells. The two layers are separated and enclosed by  $12.5 \mu\text{m}$  thick cathode foils with a Vernier pattern structure used for the precise  $z$ -coordinate determination. A (50:50) helium-ethane gas mixture is used allowing a low mass structure of only  $2.0 \cdot 10^{-3} X_0$  along the positron trajectory.

The positron time is measured by the Timing Counters (TC). Each of the two sectors (up and downstream the target) of the TC is made of  $15 \cdot 4 \times 4 \times 80 \text{ cm}^3$  BC404 plastic scintillating bars with approximately square cross-section, placed parallel to the  $z$ -axis ( $\mu$ -beam direction), along a circumference with a radius of about  $30 \text{ cm}$  from the target. Each bar is read-out at either end by a fine-mesh photomultiplier tube able to stand the spectrometer magnetic field.

The total energy of the photon as well as the time and the position are measured in a  $9001 \text{ LXe}$  calorimeter whose scintillation light is detected by  $846$  photomultiplier tubes internally mounted on all surfaces. The use of liquid xenon ensures fast response, large light yield and short radiation length.

**3.1. Trigger and data acquisition.** – All the signals coming from the detector are processed by two waveform digitizers in parallel. A  $2 \text{ GHz}$  custom digitizer (DRS [8]) is used for offline analysis and its resolution is mandatory to search for possible pile-up effects. A  $100 \text{ MHz}$  FADC-based digitizer is used for trigger purposes. It receives the

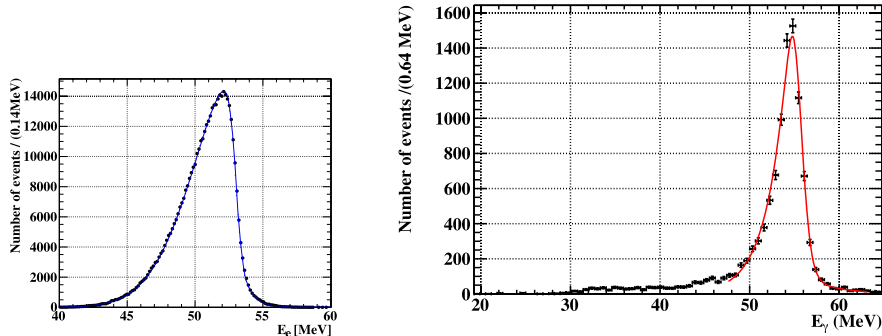


Fig. 3. – Measured Michel positron energy (left) and measured energy for 54.9 MeV photons (right). The solid lines are the respective fit functions.

signals from the LXe detector and the TC and selects on-line events with a photon energy around 52.8 MeV, a time coincident positron hit on the TC and a rough collinearity of the two particles. This reduces the flux from the initial  $3 \cdot 10^7 \mu$  decays per second to an acquisition rate of  $\sim 7$  Hz.

**3.2. Calibration.** – The performances of the detector and their stability as a function of the time have been monitored with extreme care. Standard checks have been done for the LXe temperature and pressure and the DCH gas composition and pressure. More sophisticated measurements have been routinely performed for the LXe energy calibration and the TC-LXe time synchronization. The outmost important methods for calibrating rely on the exploitation of a Cockcroft-Walton 1 MeV auxiliary accelerator. Photons of 17.67 MeV from  ${}^7\text{Li}(p, \gamma){}^8\text{Be}$  allow the calibration of the LXe energy scale (in the low energy region) while two simultaneous photons from the reaction  $\text{B}(p, \gamma)\text{C}$  detected in the LXe and TC determine the time offsets of the TC bars.

Letting a beam of negative pions impinge on a hydrogen target we took data from the charge exchange process  $\pi^- p \rightarrow \pi^0 n$  (CEX). The 54.9 MeV photons from the  $\pi^0$  decay (fig. 3) were used for the absolute energy calibration of the LXe calorimeter and to extract its energy resolution which is about 5.5% FWHM.

Positron energy scale and resolution were found by fitting the edge of the Michel spectrum on data (fig. 3). We parameterize the resolution function with a core Gaussian component (60%) with a sigma of 374 keV and two tails with sigma 1.06 MeV and 2.00 MeV contributing 33% and 7%, respectively. This performance is far from the goal and is due to the instability of the DCH in the course of the run. This problem has been solved during the 2009 shutdown.

Intrinsic time resolution of TC bars were extracted by comparing times measured in two adjacent bars by the same positron passing through. We find a value better than 60 ps. The  $t_{e\gamma}$  time resolution has been studied and monitored by taking RMD events at reduced beam intensity by relaxing the trigger requirement to include acollinear positron and photons. Moreover we are able to see the RMD  $t_{e\gamma}$  peak also during normal physics run (see fig. 4) and to estimate a time resolution for the signal of  $(148 \pm 17)$  ps.

The angular resolutions,  $\sigma_\theta = 18$  mrad and  $\sigma_\phi = 10$  mrad, were found by fitting separately two segments of the same track and propagating them to the point of closest approach to the beam axis.

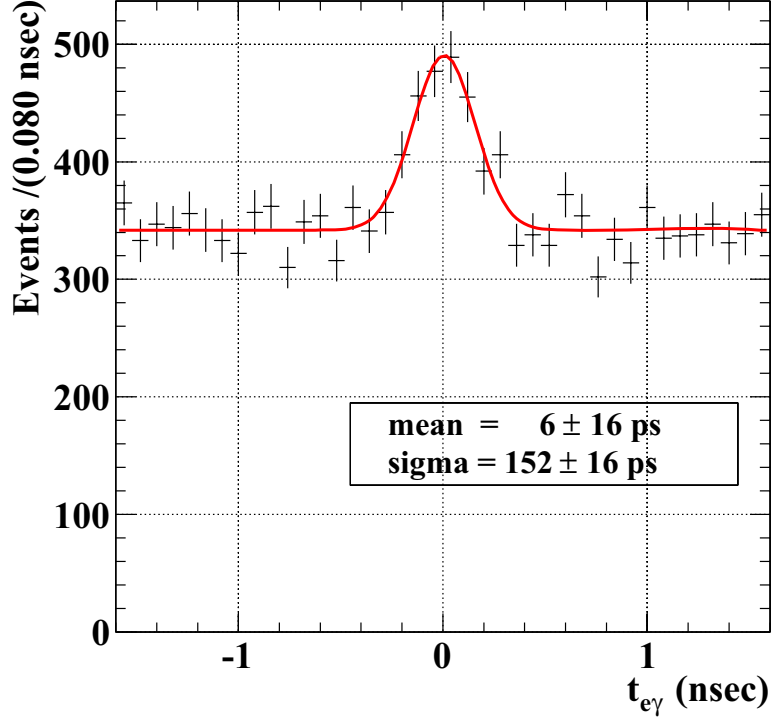


Fig. 4.  $-t_{e\gamma}$  distribution for RMD events taken during normal data taking with the selection  $40 \text{ MeV} < E_\gamma < 45 \text{ MeV}$ .

#### 4. – Data analysis and result

Thanks to the excellent performance of the PSI cyclotron, we collected data corresponding to about  $9.5 \cdot 10^{13}$  muons stopped on target in a period of 10 weeks which represents about the 10% of the total foreseen statistics. We adopt a blind analysis technique. Events with  $E_\gamma$  close to 52.8 MeV and  $t_{e\gamma}$  close to 0 were removed from the main stream until the full analysis was finalized to avoid any biases. The analysis algorithms were calibrated and validated in a large data sample in a kinematical region where no signal is expected (the sidebands) out of the blind box. The upper limit on the number of the signal events is determined by a maximum likelihood fit in the analysis region defined by  $46 \text{ MeV} < E_\gamma < 60 \text{ MeV}$ ,  $50 \text{ MeV} < E_e < 56 \text{ MeV}$ ,  $|t_{e\gamma}| < 1 \text{ ns}$ ,  $\theta_{e\gamma}, \phi_{e\gamma} < 100 \text{ mrad}$ .

An extended likelihood function  $L$  is constructed as

$$(1) \quad \mathcal{L}(N_s, N_{\text{RMD}}, N_b) = \frac{N^{\text{Nobs}} e^{-N}}{N_{\text{obs}}!} \prod_{i=1}^{N_{\text{obs}}} \frac{1}{N} [N_{\text{sig}} S + N_{\text{RMD}} R + N_b B],$$

where  $N_s$ ,  $N_{\text{RMD}}$ ,  $N_b$  are the number of the signal, RMD and accidental background events with their respective PDFs S, R and B.  $N_{\text{obs}}$  is the number ( $= 1189$ ) found in the analysis window and  $N = N_s + N_{\text{RMD}} + N_b$ . Each PDF is the product of the specific PDF associated to each variable and determined as follows. The probability density functions for the signal, the RMD and the accidental background were taken from data whenever

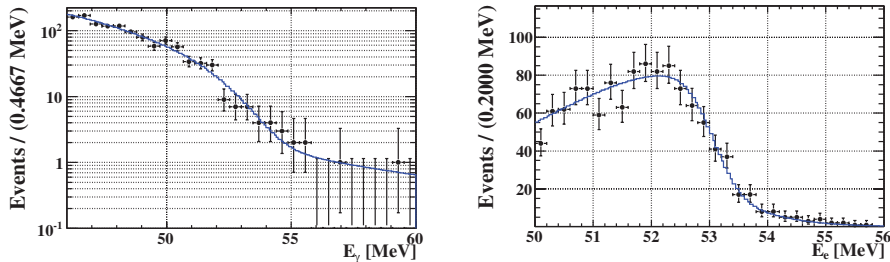


Fig. 5. –  $E_\gamma$  (left) and  $E_e$  (right) distributions for all the events in the analysis window. The line is the likelihood function fit.

possible or from Monte Carlo computations using experimental inputs. In particular for the signal  $E_\gamma$  was taken from MC,  $E_e$  and  $\theta_{e\gamma}$  from data and  $t_{e\gamma}$  from the RMD sample. For the RMD component the energies and the angle were extracted from a MC simulation based on the Kuno-Okada [9] model while  $t_{e\gamma}$  was taken from data as for the signal. Finally for the accidental background  $E_\gamma$  and  $\theta_{e\gamma}$ , were extracted from a fit to a  $t_{e\gamma}$  sideband,  $E_e$  from data and for  $t_{e\gamma}$  a flat distribution was taken. The distributions of photon and positron energies in the analysis window are shown in fig. 5, together with the projections of the fitted likelihood function.

The 90% confidence levels (c.l.) on  $N_{\text{sig}}$  and  $N_{\text{RMD}}$  are determined by the Feldman-Cousins method [10]. A contour of 90% c.l. on the  $(N_{\text{sig}}, N_{\text{RMD}})$  plane is built by a toy Monte Carlo simulation. We obtain an upper limit on  $N_{\text{sig}} < 14.7$  including the systematic error.

The largest contribution comes from the uncertainty of the selection of photon pile-up events ( $\Delta N_{\text{sig}} = 1.2$ ), the response function of the positron energy ( $\Delta N_{\text{sig}} = 1.1$ ), the photon energy scale ( $\Delta N_{\text{sig}} = 0.4$ ) and the positron angular resolution ( $\Delta N_{\text{sig}} = 0.4$ ).

The upper limit on  $\text{BR}(\mu \rightarrow e\gamma)$  is computed by normalizing the u.l. on  $N_{\text{sig}}$  to the number of Michel decay positrons counted simultaneously with the signal and using the same analysis cut and taking into account the small differences in efficiencies and acceptances. In this way, the result is independent of the instantaneous beam rate and is almost insensitive to the positron acceptance and efficiency associated with the DCH and TC.

The final result turns out to be  $\text{BR}(\mu \rightarrow e\gamma) < 2.8 \cdot 10^{-11}$  at 90% c.l. [11]. This result can be compared with the estimated sensitivity of the experiment with the available data sample. This is defined as the mean of the distribution of the upper limit computed by toy Monte Carlo simulations and assuming no signal and the same number of accidental background and RMD events as in the data. The mean of the distribution is  $1.3 \cdot 10^{-11}$ , which is comparable with the present best limit established by MEGA [2], while the probability to obtain an upper limit greater than  $2.8 \cdot 10^{-11}$  is 5%.

## 5. – Conclusions and perspectives

After a start-up engineering run in 2007 we had the first MEG physics run at the end of 2008, which suffered from detector instabilities. Data from the first three months of operation of the MEG experiment give a result which is competitive with the previous limit. During 2009 shutdown the problem with the drift chamber instability was

solved and the detector operated for all the 2009 run without degradation. Additional physics data were taken in November and December 2009 with many improvements regarding efficiency, electronics and resolutions. We are confident, therefore, in obtaining a sensitivity that should allow us to improve the present experimental limit.

\* \* \*

I am grateful to the many MEG colleagues who helped me in the preparation of the talk and of these proceedings. A special thank to the Conference Organizers that invited me to present MEG and to enjoy the beautiful slopes of La Thuile.

#### REFERENCES

- [1] BALDINI A. *et al.* (MEG COLLABORATION), Research Proposal to PSI R-99-05 (1999).
- [2] BROOKS M. L. *et al.* (MEGA COLLABORATION), *Phys. Rev. Lett.*, **83** (1999) 1521.
- [3] BARBIERI R. *et al.*, *Nucl. Phys. B*, **445** (1995) 225.
- [4] CALIBBI L. *et al.*, *Phys. Rev. D*, **74** (2006) 116002.
- [5] SAWADA R., *Nucl. Instrum. Methods A*, **623** (2010) 258.
- [6] HILDEBRANDT M., *Nucl. Instrum. Methods A*, **623** (2010) 111.
- [7] DUSSONI S. *et al.*, *Nucl. Instrum. Methods A*, **617** (2010) 387.
- [8] RITT S., *Nucl. Instrum. Methods A*, **518** (2004) 470.
- [9] KUNO Y. and OKADA Y., *Rev. Mod. Phys.*, **73** (2001) 151.
- [10] FELDMAN G. J. and COUSINS R. D., *Phys. Rev. D*, **57** (1998) 3873.
- [11] ADAM J. *et al.* (MEG COLLABORATION), *Nucl. Phys. B*, **834** (2010) 1.